Photoemission of a Quantum Cavity with a Nonmagnetic Spin Separator

C. Koitzsch,[1,*] C. Battaglia,[1] F. Clerc,[1] L. Despont,[1] M. G. Garnier,[1] and P. Aebi[1]

[1]*Institut de Physique, Université de Neuchâtel, Rue A.-L. Breguet 1, CH-2000 Neuchâtel, Switzerland*

(Received 7 October 2004; published 12 September 2005)

Quantum well states are a consequence of confinement in a quantum cavity. In this study we investigate with photoemission the influence of the interface electronic structure on the quantum well state energy dispersion in ultrathin Mg(0001) films on $W(110)$. Coupling between the sp-derived quantum well states and the substrate across the interface becomes manifest in a deviation from free electronlike dispersion behavior. Most importantly, we observe a marked level splitting, which is interpreted as due to the Rashba effect at the interface. Such an interfacial electron beam splitting on materials with strong spin-orbit coupling is an essential ingredient for novel spintronic devices. The combination of a quantum cavity with a heavy, electron reflecting substrate reveals spin-splitting effects in ultrathin films without conventional magnetism being involved.

DOI: 10.1103/PhysRevLett.95.126401 PACS numbers: 71.15.Mb, 71.20.Dg, 71.70.Ej, 73.21.Fg

Classical physics is at its limit for reduced dimensions, where the quantum regime comes into play. The wavelike nature of electrons is frequently introduced with the *particle in a box* model. The advent of molecular beam epitaxy allowed the direct investigation of this textbook example of quantum mechanics with high resolution photoemission [1,2] (and references therein). Discrete, thickness dependent energy levels [see Fig. 1(a)] originate from the finite film thickness, which permits only certain cavity eigenmodes or quantum well states, whose wavelengths (λ) form a standing wave upon reflection at the boundaries [see Fig. 1(b)]. Depending on the $E(\lambda)$ relation in the solid, these allowed wavelengths translate into discrete energy levels. [3] In a first, semiclassical approach, tunneling across the confining barriers is usually neglected. This model is frequently called in quantum mechanics textbooks a *particle in a box* with infinitely high walls [see Fig. 1(c)]. In reality, however, the barrier height is only finite and the wave function might leak to some extent over the interface barrier. Therefore the electron wave function inside the cavity has to be matched to an appropriate wave function at the cavity boundaries. The quantum well state (QWS) is (partially) reflected and has to be matched to an evanescent wave, if no coupling crystal Bloch states are available. Otherwise the matching proceeds with substrate Bloch states. One distinguishes between quantum well states (complete confinement) and quantum well resonances (partial confinement due to coupling).

If the cavity modes are tuned such that the coupling scheme switches to the resonance case (or vice versa), one expects a discontinuous change in the allowed wavelengths and corresponding energies [see Fig. 1(d)]. In this sense the quantized states probe, via their reflectivity, the energy-dependent substrate band structure.

The main purpose of this study is to show that there is another effect (not considered so far for QWS) that influences and modifies the QWS. The substrate not only perturbs the dispersion relation, it may also lead to an appreciable spin splitting of the quantum well states.

The interfacial, electron reflecting potential gradient translates, via relativistic Zeeman coupling, to an effective in-plane magnetic field, which in turn lifts the spin degeneracy. The size of this so-called Rashba splitting is given by the Hamiltonian $H_{\text{Rashba}} \sim (\vec{k} \times \nabla\vec{V}) \cdot \vec{\sigma} \sim \vec{B}_{\text{eff}} \cdot \vec{\sigma}$ [4], where σ is the Pauli spin matrix. The geometrical relation between plane wave propagation vector ($\vec{k}$), interfacial potential gradient ($\nabla\vec{V}$) direction, and the effective in-plane magnetic field (B_{eff}) is shown in Fig. 1(e). The spin splitting $E(k,\uparrow) \neq E(k,\downarrow)$ into spin-up, $\uparrow$, and spin-down, $\downarrow$ for $k_{\|} \neq 0$, however, is only possible for a broken inversion symmetry, since otherwise the Kramers degeneracy dictates $E(k,\uparrow) = E(k,\downarrow)$. Because of the presence of inversion symmetry in bulk Mg and W, the respective bulk Bloch states are not spin split. However, surface states and QWS, which do not couple to substrate Bloch states and nevertheless have strong weight at the interface, experience inversion-symmetry breaking and are subject to this effective magnetic field in the vicinity of the strong potential around the tungsten cores. In a field effect transistor the Rashba spin splitting can be tuned with an applied gate voltage leading to the concept of the spin transistor of Datta and Das [5]. Similarly the degree of wave function localization, which is, e.g., different for Mg surface states and QWS of different order, should affect the splitting as well and is therefore of fundamental interest for spintronic applications using the Rashba effect.

Thin Mg films have been grown on $W(110)$ at room temperature. The photoemission results were obtained with hydrogen Ly_{α} radiation ($h\nu = 10.2$ eV) and the sample was rotated with a motorized 2-axes goniometer stage [6]. Mg grows on W in a layer-by-layer fashion over a large thickness range and supports well-defined quantum well states [7]. All films exhibit a narrow thickness spread as revealed by the continuous evolution of the observed dis-

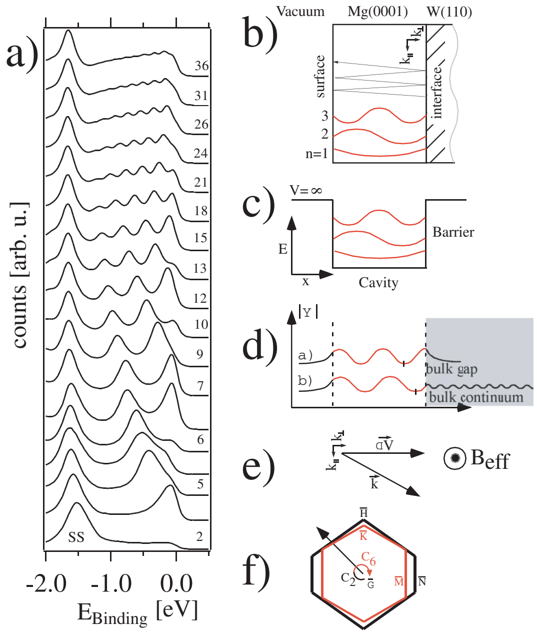

FIG. 1 (color online). (a) Quantum well states as seen by ultraviolet photoemission [modified VG Escalab MkII with a monochromatized hydrogen $Ly_\alpha(h\nu = 10.2$ eV) photon source] in normal emission geometry at $T = 300$ K. States above the surface state energy at -1.7 eV are QWS. The film thickness for the spectra is given in units of unit cells (5.21 Å), comprising two atomic layers. (b) Experimental cavity with surface and interface boundary and three cavity modes. An off-normal quantum well state, characterized by a wave vector component parallel to the surface, $k_\|$, indicating a sidewards displacement. (c) Ideal cavity with infinitely high walls. (d) Difference between a confined quantum well state and a leaky quantum well resonance with a corresponding change in wavelength. (e) Vectorial representation of the effective in-plane magnetic field, $B_{\rm eff}$, at the Rashba interface. (f) Brillouin zones with high symmetry points for the epitaxial relationship between the sixfold symmetric (C_6) Mg(0001) thin film and the twofold symmetric (C_2) $W(110)$ substrate.

crete energy levels as thickness increases [see Fig. 1(a)]. Layer-resolved films would exhibit discrete static features associated with the specific number of layers present in the film. The energy position of the quantum well states can be understood in the framework of the phase accumulation model [7]. This model expresses the condition for constructive interference in terms of phase shifts within the film of thickness d and at the surface ($\phi_{\rm surface}$) and interface boundary ($\phi_{\rm interface}$). A stationary state requires the total phase shift to be an integer times 2π, which naturally selects discrete k vectors.

$$2kd + \phi_{\rm interface} + \phi_{\rm surface} = n2\pi \qquad n \in \text{integer}. \quad (1)$$

These geometry-enforced k vectors correspond to energy values via the bulk band dispersion $E(k)$. For increasing well dimensions more states can be accommodated (Fig. 1) and the influence of the boundary conditions becomes less important, since the corresponding phase shifts are divided by the film thickness in order to obtain the allowed k vector. A possible substrate influence on the cavity modes is therefore best detected for small cavities.

Mg grows epitaxially in the [0001] direction with an in-plane orientation such that the $[11\bar{2}0]$ direction is aligned to the $[001]_{\rm bcc}$ direction of the W substrate. This relation corresponds in reciprocal space to an alignment between the $\bar{\Gamma}\bar{M}_{\rm hex}$ and $\bar{\Gamma}\bar{N}_{\rm bcc}$ high symmetry directions of the respective Brillouin zones [see Fig. 1(f)]. The $W(110)$ surface is a pseudohexagonal growth substrate [8,9] but exhibits only a twofold rotational axis. In this sense electronic overlayer states, which exhibit a reduction of symmetry from C_6 to C_2 reflect the influence of the reflectivity of the substrate. Quite naturally such a substrate influence can be detected in a full hemispherical measurement as twofold symmetric features [10].

In fact, the band dispersion of Mg is almost not affected by its weak hexagonal lattice potential and is almost free electronlike. Correspondingly, the k-resolved band structure is dominated by a parabolic dispersion relation with spheres as constant energy surfaces. The ΓMK plane of the Brillouin zone cuts the corresponding free electron parabolas in circles. The circular, isotropic in-plane dispersion relation is corroborated by *ab initio* electronic structure calculations for a freestanding three unit cell thick magnesium slab [see Fig. 2(a)]. For this thickness the well-known Mg surface state (SS) is already apparent in the calculation and cuts the Fermi level in a ringlike fashion. In contrast to this, the experiment on a film with similar small thickness [Fig. 2(b)] displays clear deviations from this ideal behavior. The experimental film thickness supports one ($n = 1$) occupied quantum well state in addition to the aforementioned surface state. The Mg surface state is clearly not

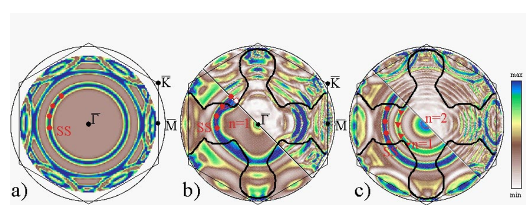

FIG. 2 (color online). Fermi surface contours displayed as a function of $k_\|$. Marked is the hexagonal Mg Brillouin zone with high symmetry points $\bar{\Gamma}$, $\bar{M}$, $\bar{K}$; SS labels free electronlike surface state and $n = 1$, 2 successive QWS; symbols are identical to the ones in Fig. 3. (a) Theoretical Fermi surface for a 3 unit cell thick slab, obtained with the APW + lo code WIEN2K [19]. (b) and (c) Experimental Fermi surface map for a three and eight unit cell thick film, respectively; experimental raw data are plotted in the lower left part (i.e., below the 135° diagonal line) and asymmetry plots [11] in the upper part; the curved black line marks the border between the surface projected bulk states and surface projected bulk gap; it falls together with strong deviations from the circular symmetry, highlighted in the asymmetry plots (see upper part). The color bar (right side) indicates the intensity scale.

cutting the Fermi level isotropically, but instead a twofold symmetry points directly to the substrate influence.

The surface state wave function probes the electronic structure of the underlying tungsten substrate and discontinuities are expected if the coupling regime changes to the resonance case upon leaving the confining substrate band gap. These locations in k space for the Fermi energy are indicated with thick black lines. If the gradient of deviations from isotropy is plotted [11] [upper part in Figs. 2(b) and 2(c)] one can clearly see that indeed the transition to the resonance case leads to discontinuities in the in-plane dispersion, which are especially pronounced at the band edges (drawn in black). If a similar measurement is inspected for a thicker, two quantum well state supporting film [Fig. 2(c), with $n = 2$], similar effects can be observed. However, in agreement with the phase accumulation model, the effects of the substrate are much weaker since the interface phase shift is less important for the total phase of a thicker film. Nevertheless, tracing the bulk band edges is still possible [12].

The electron reflection at the interface boundary might not only warp the one-electron band structure, it may have surprising effects on the spin structure as well. *Magnetic* QWS on a *ferromagnetic* substrate have already been reported [13]. However, for Mg on $W(110)$ both overlayer and substrate material are nonmagnetic, which points intuitively to spin degeneracy. Nevertheless, it has recently been reported that the high atomic number (Z) material $W(110)$ ($Z = 74$) gives rise to a zero field, spin splitting of its surface state [14,15]. The Rashba effect lifts the spin degeneracy at the surface, where inversion symmetry is broken [4].

Figure 3 shows a set of measurements obtained for increasing thicknesses, as it is reflected in the increasing number of QWS at $\bar{\Gamma}(k_{\parallel} = 0)$. The scans were obtained for an azimuthal angle of 135°, which is indicated in Fig. 2(b). Similarly, as in the previously discussed Fermi surface measurements, we note the strong influence of substrate band edges on the energy dispersion. The surface state is perturbed in Fig. 3(a) in regions close to the band edge labeled with 1 and 2, due to coupling to specific bands. However, the appearance of additional bands is very striking (open symbols), and are split off the original main quantum well peak and the surface state. The upper branch of the split surface state is clearly visible in Fig. 3(a) (open and closed circles) and becomes more faint in Fig. 3(b). The surface state splitting is only observed after the state is located in the substrate band gap and vanishes for higher thicknesses [Fig. 3(c) and 3(d)].

The behavior of the QWS emission is similar except that it extends to higher thicknesses [triangles in Fig. 3(a)–3(d)] as expected, since the QWS are delocalized over the entire film. The splitting is again only apparent in the $E(k)$ region of the substrate band gap.

The presented measurements bear interesting and important implications for one of the key parameters of the

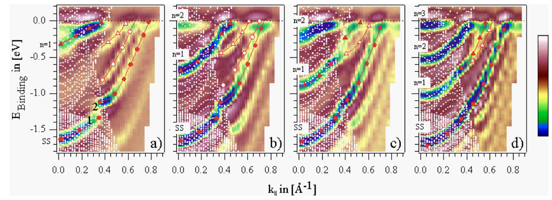

FIG. 3 (color online). $E(k_{\parallel})$ dispersion plots for 4, 6, 8, and 11 unit cell thick films taken along the 135° diagonal line (Fig. 2) are displayed in (a), (b), (c), and (d), respectively. Consecutive QWS $n = 1$, 2, 3 and the surface state (SS) are labeled. The second derivative of the measurements is shown to highlight the different features. The surface projected band structure of $W(110)$ appears as an overlay of white dots. Empty and filled circles mark the surface state and its splitting; empty and filled triangles label the $n = 1$ QWS and its splitting.

particle in the box model, namely, the interfacial electron reflectivity. The leakage to the substrate is low for both, truly confined quantum well states and partially confined quantum well resonances. This is probably due to unfavorable symmetry-forbidden coupling between quantum well resonances and substrate states. Nevertheless, substrate band edges can be detected as perturbations in the in-plane dispersion. This demonstrates that the interfacial phase shift depends on the specific energy-, k-vector-, and symmetry-dependent matching conditions. Present empirical models which compute the energy-dependent phase shift in terms of the distance to the band edge do not describe this system correctly. A scalar value for the interfacial phase shift does not reproduce all properties of the involved matched wave functions.

Full hemispherical measurements, as shown here, are particularly advantageous for QWS spectroscopy on low symmetry substrates because a symmetry breaking is directly observed in the measurements. Furthermore, the measurements do not rely on the exact knowledge of the prepared thickness. This is especially important for QWS that is not layer resolved.

The most important finding on the confined states is, however, the observed splitting. We would like to point out, that, in contrast to Matsuda *et al.* for Ag/Si(001) [16], we observe a splitting primarily in gap regions of the substrate. Therefore, an explanation of the splitting as due to a partial confinement by the substrate continuum does not hold. Similarly, structural deviations, e.g., different domains or a lattice mismatch between film and substrate, are not expected to yield discontinuities at substrate band edges [7]. Such a dependence on the k-resolved substrate band structure points to an electronic effect, where the high atomic mass of the $W(110)$ substrate leads to relativistic effects expressed by the Rashba term. The lack of inversion symmetry across the interface or more appropriately the lack of inversion symmetry and a concomitant lifting of the Kramers degeneracy at the confining barrier leads to a spin splitting. The effect is smaller or absent for states which hybridize with substrate states. Hybridization implies loss of their surface (interface) character and accumulation of bulk character with inversion symmetry [Fig. 1(d)]. On the other hand, only the potential of the tungsten nuclei gives rise to a sizeable spin splitting [17]. For this reason, the surface state is not spin split anymore for large thicknesses [Fig. 3(c) and 3(d)]. The surface state wave function decays exponentially towards the interface and therefore interface effects become less important for thick films. The magnitude of the observed splittings is with some hundred meV in the same range as the spin-orbit splitting of the W $5d$ band. The Rashba Hamiltonian predicts a vanishing spin splitting for $k_{\|} = 0$ and an increase with increasing $k_{\|}$ for a uniform gradient of the potential barrier. However in this case the barrier itself is profoundly k dependant and therefore simplified model calculations are not applicable. The position inside the gap of the projected W band structure might not only influence the size of the splitting, but might also be responsible for the observed intensity differences of the respective upper and lower branches.

The observation of such a spin splitting requires a heavy substrate with a large atomic spin-orbit splitting parameter (expressed by a strong potential gradient) [Fig. 1(d) and 1(e)], combined with inversion-symmetry breaking at the interface. These requirements might explain why this relativistic effect has not been observed for quantum cavities so far. The presented data indicate that a heteroepitaxially formed two-dimensional electron gas is subjected to a spin splitting due to the presence of an interface. Strict two-dimensional surface systems [15] are fixed in their geometry and hence energy. Instead within this three-dimensional approach, issues like the effect of localization, energy tuning and band curvature of QWS on the spin-orbit splitting might be separately addressed.

The described system also bears a striking resemblance to spin-split final-state effects in photoemission, as described by Kirschner *et al.* [18]. They observed an inherent spin polarization of the photoemission signal due to the matching of the Bloch spinor wave function to the free electron spinor wave function of the outgoing photoelectron. In the present case the matching between the spin-orbit split spinor regime of the substrate and the free electron spinor regime of the quantum well cavity proceeds over the interface and appears to introduce a net spin splitting as well.

The effects of a Rashba interface on QWS are crucial ingredient for spintronic devices, such as the spin transistor proposed by Datta and Das [5]. For this type of device, the critical question is how the change of carrier localization at the interface due to a gate voltage affects the channel spin separation. However, the present study indicates that the spin splitting is inherently dependent on the detailed k-resolved electronic structure at the interface. Therefore a one-dimensional approximation of the involved material band structures with essentially the upper band edge as parameter might not be sufficient for device design purposes. Instead a complete modelling of the interface electronic structure seems necessary to predict the k-resolved spin splitting. The bulk inversion symmetry of both Mg and W (in contrast to common semiconductors) opens up interesting new possibilities to study spin relaxation in these quantum well structures.

We are greatly indebted to our workshop and electric engineering team. Financial support by the Fonds National Suisse pour la Recherche Scientifique is gratefully acknowledged. Valuable scientific discussions with P. Blaha are acknowledged.

*Electronic address: http://www.unine.ch/phys/
Email address: Christian.Koitzsch@gmx.ch

[1] J. Paggel, T. Miller, and T.-C. Chiang, Science **283**, 1709 (1999).
[2] T.-C. Chiang, Surf. Sci. Rep. **39**, 181 (2000).
[3] The wave vector vs wavelengths relation is given by $\lambda = \frac{2\pi}{|\vec{k}|}$. The wave vector $\vec{k}$ is decomposed into a component parallel to the film, $k_{\|}$, and a component perpendicular to the film, $k_{\perp}$. There is no lateral confinement for the film and $k_{\|}$ is quasicontinuous. Because of reduced thickness, $k_{\perp}$ is quantized. Each state is therefore characterized by the energy dispersion relation $E(k_{\perp \text{quantized}}, k_{\|})$.
[4] E. Rashba, Fiz. Tverd. Tela (Leningrad) **2**, 1224 (1960); [Sov. Phys. Solid State **2**, 1109 (1960)].
[5] B. Datta and S. Das, Appl. Phys. Lett. **56**, 665 (1990).
[6] P. Aebi, J. Osterwalder, P. Schwaller, L. Schlapbach, M. Shimoda, T. Mochiku, and K. Kadowaki, Phys. Rev. Lett. **72**, 2757 (1994).
[7] F. Schiller, M. Heber, V. Servedio, and C. Laubschat, Phys. Rev. B **70**, 125106 (2004).
[8] J. Hayoz, S. Sarbach, T. Pillo, E. Boschung, D. Naumovic, P. Aebi, and L. Schlapbach, Phys. Rev. B **58**, R4270 (1998).
[9] L. A. Bruce and H. Jaeger, Philos. Mag. A **38**, 223 (1978).
[10] A structural deformation of the film due to stress/strain can be excluded on the basis of low energy electron diffraction and x-ray photoelectron diffraction measurements, which are not presented here.
[11] The anisotropy plot has been obtained from the measured data by subtracting and normalizing to the circular average and plotting the gradient.
[12] L. Aballe, C. Rogero, P. Kratzer, S. Gokhale, and K. Horn, Phys. Rev. Lett. **87**, 156801 (2001).
[13] J. E. Ortega, F. J. Himpsel, G. J. Mankey, and R. F. Willis, Phys. Rev. B **47**, 1540 (1993).
[14] E. Rotenberg, J. Chung, and S. Kevan, Phys. Rev. Lett. **82**, 4066 (1999).
[15] M. Hochstrasser, J. Tobin, E. Rotenberg, and S. Kevan, Phys. Rev. Lett. **89**, 216802 (2002).
[16] I. Matsuda, T. Ohta, and H. Yeom, Phys. Rev. B **65**, 085327 (2002).
[17] L. Petersen and P. Hedegård, Surf. Sci. **459**, 49 (2000).
[18] J. Kirschner, R. Feder, and J. Wendelken, Phys. Rev. Lett. **47**, 614 (1981).
[19] P. Blaha, K. Schwarz, G. Madsen, D. Kvasnicka, and J. Luitz, computer code WIEN2K, Technische Universität Wien, 2001, ISBN 3-9501031-1-2.